Position Estimation of Outer Rotor PMSM Using Linear Hall Effect Sensors and Neural Networks

Yuyao Wang
Electrical and Computer Engineering
University of Illinois Urbana-Champaign
Champaign, IL, USA
yuyaow2@illinois.edu

Yovahn Hoole
Electrical and Computer Engineering
University of Illinois Urbana-Champaign
Champaign, IL, USA
yhoole2@illinois.edu

Kiruba Haran
Electrical and Computer Engineering
University of Illinois Urbana-Champaign
Champaign, IL, USA
kharan@illinois.edu

***Abstract*—A position estimator for an outer rotor permanent magnet synchronous machine (PMSM) is presented and evaluated. This proposed estimator uses a machine-learning based neural network algorithm to interpret the signals, which are obtained from linear Hall-effect sensors located in the fringe field of the rotor. The main objective is to design a cost-effective position estimation system that is comparable to encoders and resolvers in functionality and performance, without the limitations of sensorless position estimation methods. Learning signal data sets are acquired with commercial sensors and an outer rotor PMSM, and offline training steps and results are discussed.**

***Index Terms*—permanent magnet synchronous machine, PMSM, position estimation, neural network, Hall effect sensor**

I. Introduction

In recent years, there has been an ongoing push for electrification of transportation, with the proliferation of electric vehicles such as bicycles and cars. Most of these vehicles rely on electric motors to provide the driving force, and out of the motor options available, the permanent magnet synchronous machine (PMSM) is an attractive option due to the high specific power arising from the use of permanent magnets. To use PMSMs in electric aircraft, further improvements to the specific power are required, in which one approach is to increase the operating frequency and pole count while adopting an air core topology to reduce iron in the machine [1].

To extract the peak performance out of PMSMs, the control and drive system requires an accurate position feedback of the rotor angle in order to align the current vector and achieve maximum torque output. Traditionally, this was fulfilled by the integration of a position transducer with the motor shaft, such as an encoder or resolver, which increases the cost and mechanical complexity of the system. An alternative to the transducers is the use of sensorless techniques, which can be broadly classified into two main categories, those based on measurement of the back-emf of the motor [2] [3], and those based on high-frequency signal injection into the motor [4]–[8]. However, back-emf based methods are unable to estimate the rotor position accurately at low speeds due to reduced signal amplitudes. While the signal injection based methods will work well at low and zero speeds, these rely on either the inherent saliency in the machine, or anisotropy due to saturation effects in non-salient machines. In the intended target machine [1], the use of air core topology results in no inherent saliency, while the reduction of iron yoke and the large magnetic air-gap reduces the effects of local anisotropy on induced saliency. This results in additional difficulties in the implementation of sensorless techniques that will work well at low speeds. Conversely, the presence of an outer rotor provides easy access to measurements of the leakage magnetic flux on the outside of the machine, which is also relatively shielded from the magnetic flux produced by the stator windings while the machine is in operation. Therefore, it is possible to use linear Hall effect sensors to measure the external leakage magnetic flux of the rotor. This provides an alternative that is easier to implement than the sensorless methods, which is also able to operate at low and zero speeds and is cheaper than the inclusion of a position transducer. [9] used two linear Hall effect sensors located 90 electrical degrees apart to measure the edge fields of a PMSM rotor, which is passed into an adaptive notch filter to filter out harmonics and a phase-locked loop (PLL) to obtained speed and angle estimates. This method managed to achieve an error of less than 3 degrees. [10] measured the rotor flux using three low resolution Hall effect sensors in conjunction with a support vector machine algorithm, which allowed the estimation error to be reset every 60 electrical degrees and achieved a starting torque in the range of 86.6% to 100% of the maximum torque. [11] used two linear Hall effect sensors measuring the leakage flux from one end of the rotor and processed the signals using two synchronous frequency extractors, which allowed for estimation error within 3.8 degrees when applied to a magnetically suspended PMSM.

This paper proposes the use of multiple Hall effect sensors and a data-driven neural network model to process the sensor readings. The neural net will be trained against the ground-truth readings obtained from an attached resolver. A data-driven model is chosen for its generalizability, as this allows for the model to be tuned and calibrated for various motors and scenarios with a short calibration phase, removing the need to separately obtain the transfer function for each system. A neural network based model is chosen for its extensibility, which

Funding provided by the Grainger Center for Electric Machinery and Electromechanics (CEME) and the Center for Power Optimization of Electro-Thermal Systems (POETS)

978-1-5386-9350-6/19/$31.00 ©2019 IEEE

allows for easier adaptation to online learning approaches and can also be easily extended to a recurrent neural network model as described in section III.

One issue with measuring the radial leakage flux is that the flux external to the rotor is not purely sinusoidal across the circumference of the rotor. While close to being sinusoidal, the placement and geometry of the permanent magnets leads to distortions in the ideal sinusoidal relationship between the angle and the leakage flux that vary based on the motor. As a result, a robust model must be able to represent the relationship regardless of the distortions that vary from motor to motor without extensive modeling of the leakage flux from the motor. The distortions introduced by the external flux give neural networks the upper hand over curve fitting where the function to fit to must be known beforehand.

The paper is organized as follows: section II introduces the measurement setup and data collection process. section III explains the models used and the training methods. section IV and V presents the results and conclusions that can be drawn.

II. Data Acquisition Setup

With the intended target machine still in the manufacturing process, an alternative low power motor with comparable specifications and design is used for data collection and neural network validation. Specifications of the motor are shown in Table I. For the sensors, ten units of DRV5053PAQLPGM linear Hall effect sensors are mounted in a Delrin fixture which is used to position the sensors evenly spaced in an arc 2 mm above the surface of the rotor, shown in Fig.1. Ground-truth readings are obtained from an LTN RE 21-1-A01 resolver attached to the shaft of the motor, which is excited and sampled by AD2S1210 resolver-to-digital converter (RDC). A TMS320F28377D microcontroller samples the sensors and RDC at regular time intervals and collates the samples into time-series datasets for offline training of the neural network.

TABLE I
Test PMSM Specifications

Model	ThinGap TG7150
Max continuous power	4.04 kW
Max speed	10300 rpm
Max torque	4.83 Nm
Poles	32

III. Neural Network Models

A. Shallow Neural Network

In implementing the shallow neural network model, the primary objective is to create an accurate mapping from the voltage response of the Hall effect sensors to the electrical angle of the rotor. As such, the neural network model used in this study is a shallow neural network with one hidden layer composed of 100 neurons.

As can be seen in Fig.2, for a given electrical angle there is a largely deterministic voltage response from the Hall effect sensors. This can be further established with Fig.3, which

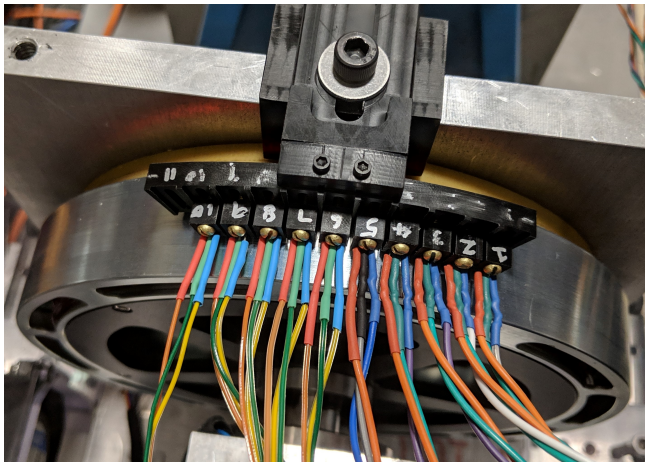

Fig. 1. Mounting of Hall effect sensors above the rotor surface

shows that for a given electrical angle, on average, a deviation of less than 2% from the mean of all samples taken at that angle is observed. This is to be expected since the fringe fields are an intrinsic characteristic of the rotors permanent magnets and the environment. Using the cosine and sine of the angle, it is then easy to form a one to one mapping between the voltage responses of the Hall effect sensors and the electrical angle. It is important to note here that while shallow neural network might simply memorize the transfer function, it can independently learn the transfer in a brief calibration period without the need for the precise parameter engineering needed required in physical models.

Since deterministic outputs are expected, the need for generalizability is largely reduced, and a high capacity model with the ability to memorize the structure of the training dataset is well suited for this application. Wide and shallow neural networks, which struggle with generalization (in comparison to deeper neural networks), are very good memorizers [12]. Given that it is possible to simulate every possible input to output pair, simple memorization of the data proves to be adequate as can be seen in Section IV.

B. Recurrent Neural Network

The recurrent neural network (RNN) model used in this study is an autoregressive model composed of one hidden layer of 20 neurons. It is modeled by the equation:

$$\theta(t) = F(\theta(t-1), \theta(t-2), B(t), B(t-1), B(t-2)) \quad (1)$$

Here $\theta(t)$ is the predicted angle at time t and B is a vector of the voltage responses of the Hall effect sensors. The motivation for the use of an RNN is derived from the temporal structure of the data, which can be seen in Fig.4 showing a plot of the change voltage output over time when the rotor is spun in a counter-clockwise direction. The voltage output of the sensors corresponds to the magnitude of the leakage flux, which changes due to the rotation of the rotor and can be directly correlated to the angle of the rotor.

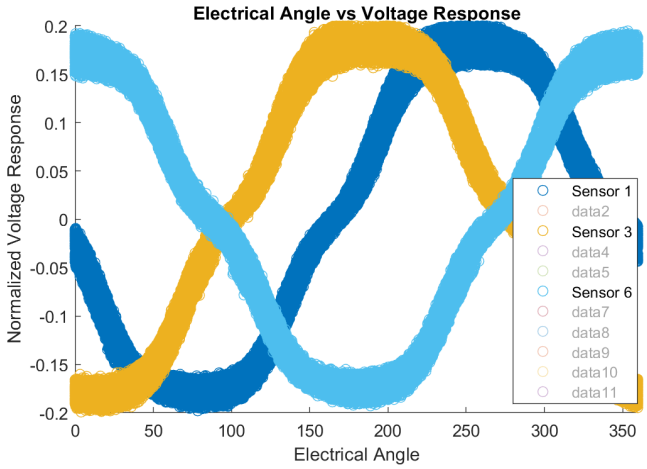

Fig. 2. Sensor voltage response vs rotor electrical angle (3 of 10 sensors)

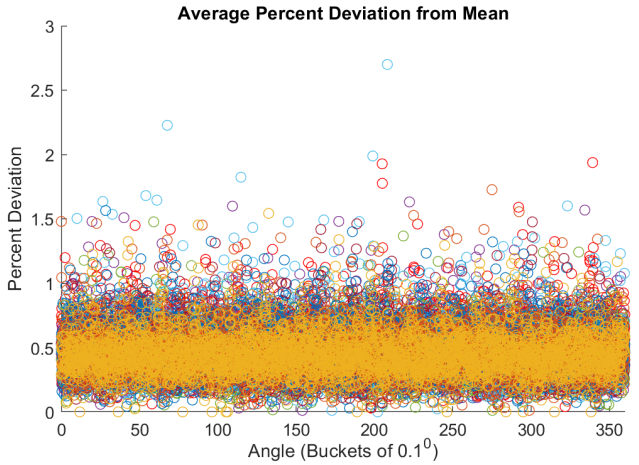

Fig. 3. Average percent deviation of samples

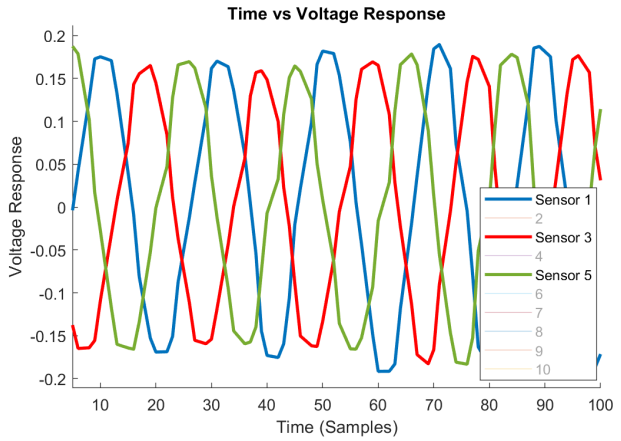

Fig. 4. Sensor voltage response vs time (3 of 10 sensors)

As can be seen, there is a strong correlation between the previous output angle and current angle. Intuitively this is expected since there are physical constraints on how far the rotor can rotate between samples.

C. Training Procedure

There are seven primary datasets that were collected. These measurements are taken under varying conditions and contain as features the time the sample was taken, mechanical angle and the readings from the 10 Hall effect sensors. Two parameters distinguish each dataset, rotational speed and rotational direction. For rotational speed, the datasets had either fast (∼300 RPM), slow (∼100 RPM) or varying (100 to 300 RPM) speeds. For rotational direction, the datasets had either clockwise (CW), counterclockwise (CCW) or varying (CW and CCW rotations within the same dataset) directions. Each of these datasets is referenced in the plots below by a Speed Direction word pair. For example Fast CCW references the dataset of samples spun in the clockwise direction at approximately 300 RPM.

To train the neural network models, each dataset is randomly split into 3 subsets with a training : testing : validation ratio of 70:15:15 in terms of the number of samples contained in each. Since the temporal structure is not necessary for the shallow neural network model, the dataset is split randomly and the order of the samples is not preserved. Thus, 70% of the data is used for training, 15% for testing and 15% for validation. Conversely, the recurrent neural network model requires sequential order to be maintained. As such, the data is split such that the first 70% is used for training, the next 15% for validation and the final 15% for testing.

Additionally, due to the nature of angles, an electrical angle of 0 degrees and 360 degrees would be classified differently with a large error if the conventional representation of degrees or radians is used. To resolve this, the sine and cosine of the electrical angle are used for training, after which the predicted electrical angle is obtained by taking the arctangent of the sine and cosine outputs of the neural networks. The Levenberg-Marquardt method was then employed to optimize the weights of both networks.The Levenberg-Marquardt algorithm finds the minimizers β, which minimizes the sum of the squares of the deviation between the predicted and ground truth values for the electrical angle. β is computed as follows [13]:

$$\beta_{min} = argmin_{\beta} \sum_{i=1}^{n} [y_i - f(x, \beta)]^2 \tag{2}$$

Where β is the set of the artificial neural networks weights and biases, n is the number of observations, y_i is the observed values of the electrical angle for the i^{th} observation, x_i is the normalized magnitudes of the leakage flux for the same observation, and the function $f(x, \beta)$ is the electrical angle predicted by the artificial neural network.

IV. Results

The best performance we can expect is ultimately limited by the uncertainty introduced by the precision of the resolver

and the RDC. The resolver has an precision of $\pm$ 0.0167 mechanical degrees, while the RDC has an precision of $\pm$ 0.022 mechanical degrees, which converts to 0.267 and 0.35 electrical degrees respectively.

The preliminary results shown here demonstrate the viability of rotor position estimation based on Hall effect sensors and a neural network-based model. Fig.5 shows the mean error of both models trained on the Slow CCW dataset and tested on all datasets. The shallow neural network model consistently demonstrates performance of around 1 electrical degree of mean error, whereas the RNN only does well on the Slow CCW dataset and the Varying CCW dataset.

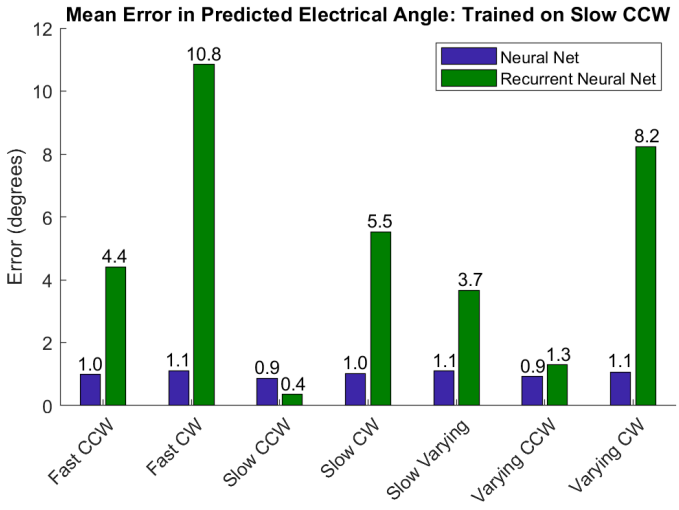

Fig. 5. Mean error when trained with the Slow CCW dataset

The shallow neural network model proves to be robust to the speed and the direction of rotation, with the distribution of the prediction errors shown in Fig.6. The distribution shows that around 60% of the samples have an error less than the mean of 1.1 degrees. 90% have an error less than 2.5 degrees, and only 5% have an error greater than the 3 degrees. The maximum error encountered by the shallow neural network model was 11 electrical degrees in this case, but several of the samples with large estimation errors only occur once in the entire dataset, and may thus be attributed to noise in the signals. More experiments and modifications to the data acquisition setup is required to verify and reduce the effects of noise on the system.

The recurrent neural network model has substantially degraded performance, and is shown to be sensitive to the speed and direction of rotation. To see if training the model on data that has both rotation directions improves performance, both models were trained on the Slow Varying dataset. The results, seen in Fig.7, show substantially improved performance on all datasets except for Fast CCW, Fast CW, and Varying CW for recurrent neural network model. Since the rotor was driven only at slow speeds in the training dataset, the model was not able to perform well on datasets taken at higher speeds,

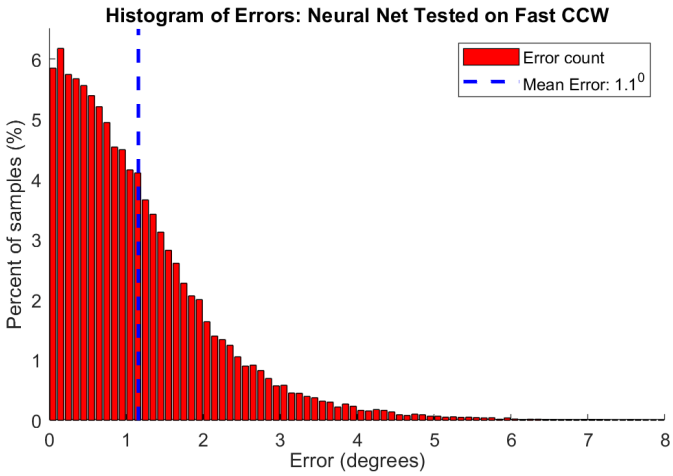

Fig. 6. Distribution of prediction error for shallow neural network

especially in the case of Fast CW where a 36.2 degree mean error is observed.

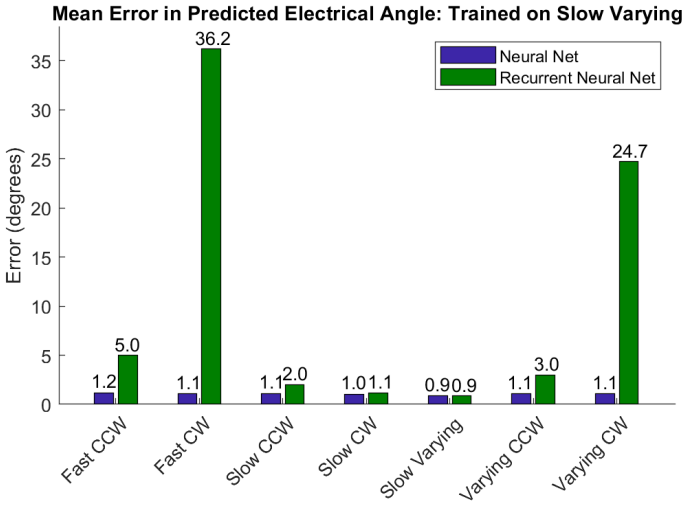

Fig. 7. Mean error when trained with the Slow Varying dataset

Finally, Fig.8 shows the distribution of errors when the recurrent neural network model was trained on the Slow CCW dataset and tested on the Fast CCW dataset. Approximately 60% of the samples have an error less than the mean of 5.0 degrees 90% have an error less than 10.5 degrees and only 5% have an error greater than 12 degrees. The maximum error encountered by the recurrent neural network model was 24.2 degrees.

For the recurrent neural network model, the inclusion of temporal data, and thus speed and direction as variables, make the problem no longer deterministic and thus memorization of the structure is no longer adequate. However, with further tuning and a more encompassing dataset, the recurrent neural network model has the potential to outperform the shallow neural net model.

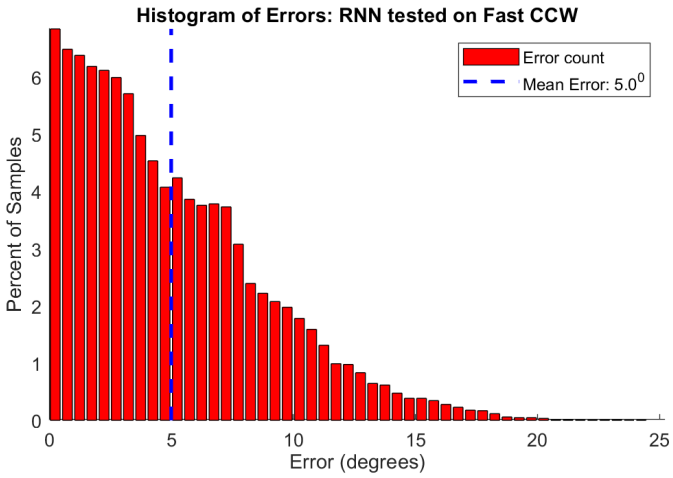

Fig. 8. Distribution of prediction error for recurrent neural network

Fig.9 shows a snapshot of the estimated angle from the shallow neural network algorithm compared with the ground truth readings obtained from the resolver and RDC system.

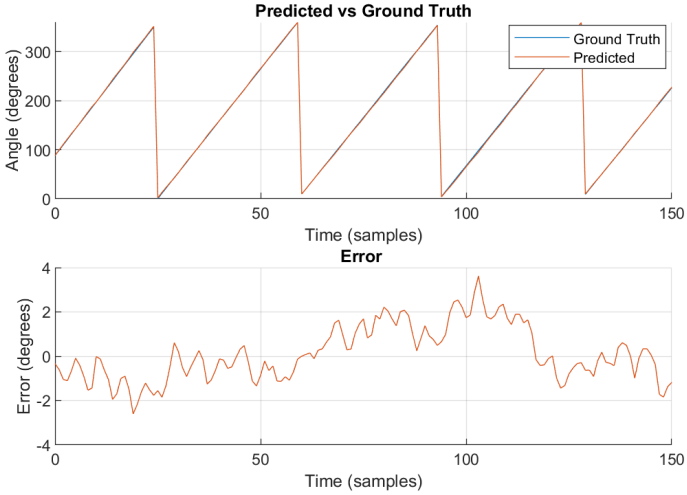

Fig. 9. Estimated Angle compared Ground Truth Angle (RDC) and Estimation Error

As an additional experiment, the number of sensors used to train both models was varied to understand the effect the number of sensors has on neural network performance. Fig.10 shows a linear decrease in mean error as the number of sensors is increased up to 9 sensors. The degraded performance with 10 sensors may be attributed to random noise in this instance, however additional testing is required to conclude whether the addition of more sensors will yield better results.

These results establish the feasibility of using a neural network based algorithm to process Hall effect sensor data to extract rotor angular information. Practical applications of this method would experience more sources of noise, both from the surroundings and from the operation of the motor. Additional testing with the introduction of various kinds of noise will be required to verify the robustness of the proposed approach.

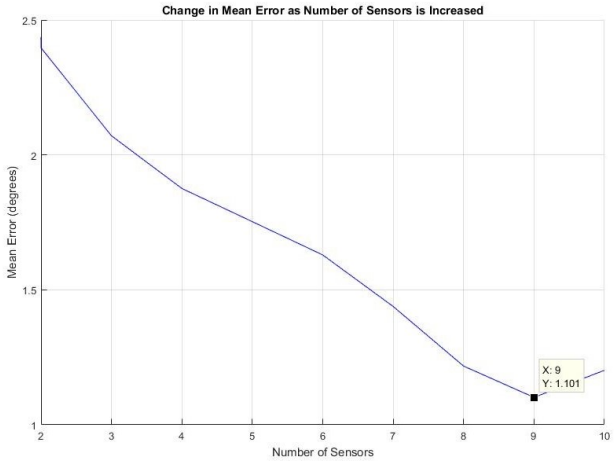

Fig. 10. Change in Mean Error as Number of Sensors is Increased

V. Conclusion

A method to estimate rotor position using linear Hall effect sensors and neural networks is investigated in this paper. Initial results from offline training of both models are promising, with consistently low mean errors lesser than 1.5 electrical degrees using a shallow neural network. Furthermore, the neural network models improve in performance in response to increased sensor count, which has the added benefit of increasing system reliability. This method has the advantage being easy to retrain in response to changes in the operating environment, such as loss of sensor units or changes in the sensor arrangements.

There is also the potential of training the neural network algorithm with rotor angle estimations obtained from sensorless back-emf methods at high speeds, and using the algorithm to augment and improve on the performance of the back-emf method at low speeds where it suffers from poor performance due to the reduced signal amplitudes.

References

[1] A. Yoon, Xuan Yi, J. Martin, Yuanshan Chen and K. Haran, "A high-speed, high-frequency, air-core PM machine for aircraft application," 2016 IEEE Power and Energy Conference at Illinois (PECI), Urbana, IL, 2016, pp. 1-4.

[2] F. Genduso, R. Miceli, C. Rando and G. R. Galluzzo, "Back EMF Sensorless-Control Algorithm for High-Dynamic Performance PMSM," in IEEE Transactions on Industrial Electronics, vol. 57, no. 6, pp. 2092-2100, June 2010.

[3] H. Kim, J. Son and J. Lee, "A High-Speed Sliding-Mode Observer for the Sensorless Speed Control of a PMSM," in IEEE Transactions on Industrial Electronics, vol. 58, no. 9, pp. 4069-4077, Sept. 2011.

[4] M. J. Corley and R. D. Lorenz, "Rotor position and velocity estimation for a salient-pole permanent magnet synchronous machine at standstill and high speeds," in IEEE Transactions on Industry Applications, vol. 34, no. 4, pp. 784-789, July-Aug. 1998.

[5] S. Ogasawara and H. Akagi, "Implementation and position control performance of a position-sensorless IPM motor drive system based on magnetic saliency," in IEEE Transactions on Industry Applications, vol. 34, no. 4, pp. 806-812, July-Aug. 1998.
[6] S. Ogasawara and H. Akagi, "An approach to real-time position estimation at zero and low speed for a PM motor based on saliency," in IEEE Transactions on Industry Applications, vol. 34, no. 1, pp. 163-168, Jan.-Feb. 1998.
[7] A. Consoli, G. Scarcella and A. Testa, "Industry application of zero-speed sensorless control techniques for PM synchronous motors," in IEEE Transactions on Industry Applications, vol. 37, no. 2, pp. 513-521, March-April 2001.
[8] Hyunbae Kim and R. D. Lorenz, "Carrier signal injection based sensorless control methods for IPM synchronous machine drives," Conference Record of the 2004 IEEE Industry Applications Conference, 2004. 39th IAS Annual Meeting., Seattle, WA, USA, 2004, pp. 977-984 vol.2.
[9] S. Jung, B. Lee and K. Nam, "PMSM control based on edge field measurements by Hall sensors," 2010 Twenty-Fifth Annual IEEE Applied Power Electronics Conference and Exposition (APEC), Palm Springs, CA, 2010, pp. 2002-2006.
[10] A. Lidozzi, L. Solero, F. Crescimbini and A. Di Napoli, "SVM PMSM Drive With Low Resolution Hall-Effect Sensors," in IEEE Transactions on Power Electronics, vol. 22, no. 1, pp. 282-290, Jan. 2007.
[11] X. Song, J. Fang and B. Han, "High-Precision Rotor Position Detection for High-Speed Surface PMSM Drive Based on Linear Hall-Effect Sensors," in IEEE Transactions on Power Electronics, vol. 31, no. 7, pp. 4720-4731, July 2016.
[12] Goodfellow, I., Bengio, Y. and Courville, A. (2017). Deep learning. Cambridge, Mass: The MIT Press, pp.108-114.
[13] Mathworks.com. (2019). Least-Squares (Model Fitting) Algorithms- MATLAB & Simulink. [online] Available at: https://www.mathworks.com/help/optim/ug/least-squares-model-fitting-algorithms.html#f204 [Accessed 28 Mar. 2019].